Climate signals in high elevation tree-rings from the semiarid Andes of north-central Chile: Responses to regional and large-scale variability

Jonathan Barichivich [a,*], David J. Sauchyn [b], Antonio Lara [a,c]

[a] Laboratorio de Dendrocronología, Instituto de Silvicultura, Facultad de Ciencias Forestales, Universidad Austral de Chile, Casilla 567, Valdivia, Chile
[b] Prairie Adaptation Research Collaborative, University of Regina, Regina, Saskatchewan, Canada S4S 7J7
[c] FORECOS Nucleus (Forest Ecosystemic Services to Aquatic Systems under Climatic Fluctuations), Millennium Scientific Initiative Nucleus of the Ministry of Planning, Chile

ARTICLE INFO

ABSTRACT

In South America, the arid and semiarid subtropical regions through the Atacama Desert and north-central Chile between 19° and 32°S are currently a gap in the tree-ring chronology network. Only a short tree-ring chronology has been published for this vast region and little is known about the suitability of many woody species for tree-ring analysis and dendroclimatology. In this paper we present the first detailed analysis of the climate responses and influences of the El Niño-Southern Oscillation (ENSO) and the Pacific Decadal Oscillation (PDO) on the tree-rings of three species new to dendrochronology and that typically occur at high elevations in the Andes of central and north-central Chile. Three well-replicated tree-ring chronologies of *Kageneckia angustifolia*, *Proustia cuneifolia* and *Fabiana imbricata* are compared with century-long regional records of precipitation and temperature, and with the N3.4 SST and PDO indices in both time and frequency-domains using correlation and wavelet analysis. The radial growth of these species is controlled by winter precipitation and is also positively correlated with temperature during most of the rainy season from April to September (autumn–spring). The regional climate as well as tree growth is strongly modulated by ENSO and ENSO-like conditions in the equatorial Pacific at both interannual and interdecadal timescales. The decadal and interdecadal variability is not correlated with PDO and appears to be related to the Interdecadal Pacific Oscillation (IPO), a Pacific-wide ENSO-like mode of climate variability. Despite their relatively short lifespans, these three new species have a high potential for dendrochronological and dendroclimatic studies in the semiarid region of Chile over the last two centuries.

© 2008 Elsevier B.V. All rights reserved.

1. Introduction

In South America, the tree-ring research during the last decades has produced important advances in the understanding of climate variability, ecology and forest management in a range of ecosystems from temperate to tropical regions. Over 200 tree-ring chronologies have been developed in Chile and Argentina, mainly of long-lived or high altitude temperate trees such as *Fitzroya cupressoides*, *Austrocedrus chilensis* and *Nothofagus pumilio* (Villalba, 2000). However, there are important tropical and subtropical gaps in the existing chronology coverage because it is discontinuous and strongly biased to mid-latitudes (~35°–43°S) of the temperate Andes of Chile and Argentina (Luckman and Boninsegna, 2001; Lara et al., 2005). This unbalanced distribution of tree-ring records is mostly due to the wood anatomy complexity and lack of distinct annual tree-rings in tropical species due to absent or weak climate or environmental seasonality (Boninsegna et al., 1989). Nevertheless, the strong rainfall and moisture seasonality in the tropical and subtropical arid regions along the Andes of Argentina, Bolivia, Peru and Chile induces the formation of well-defined annual

tree-rings in several of the woody species (Villalba et al., 1985; Roig et al., 2001; Morales et al., 2001; López et al., 2005; Rodríguez et al., 2005). These conditions have enabled the expansion of the tree-ring network into the subtropics. For instance, rainfall-sensitive chronologies of *Juglans australis*, *Cedrela lilloi*, and *Prosopis ferox* extending back over 350 years have been successfully developed in the subtropical montane forests in northwestern Argentina between 22° and 28°S (Villalba et al., 1985; 1987; 1992; 1998; Morales et al., 2004). More recently, a network of well-replicated and century-long moisture-sensitive chronologies from the world's highest forests of *Polylepis tarapacana* has been developed in the semiarid Altiplano plateau of Bolivia, Argentina and Chile at ~4000–5200 m between 16 and 22°S (Argollo et al., 2004; Moya, 2006; Solíz et al., 2009-this issue; Christie et al., 2009-this issue). Chronologies for the related species *Polylepis pepei* have also been developed at lower and more humid elevations of Bolivia at 17°S (Roig et al., 2001). Recent work in Peru has produced short ENSO-sensitive chronologies of *Bursera graveolens* in the dry forests of northwest Peru between 3° and 7°S (Rodríguez et al., 2005) and *Prosopis pallida* along the Peruvian Desert between 5° and 14°S (López et al., 2005; 2006). In addition, other species such as *Eryotheca ruizii* and *Cordia lutea* have proven to be suitable for dendrochronological work in northwestern Peru (Rodríguez et al., 2005).

* Corresponding author. Tel.: +56 63 221566; fax: +56 63 221230.
E-mail address: J.Barichivich@uea.ac.uk (J. Barichivich).

Despite these recent developments in subtropical tree-ring research, the arid and semiarid subtropical regions through the Atacama Desert, and north of the Mediterranean region of central Chile from 19° to 32°S, remain as a major gap in the tree-ring chronology coverage along the west coast of South America (Lara et al., 2005; see Fig. 1a). Only a short tree-ring chronology of *Prosopis chilensis* at 29°38′S (López et al., 2006) has been published for the area. This is a key region to examine the influences of ocean/atmosphere processes (e.g. El Niño) on climate and water availability and how these extremely sensitive and threatened ecosystems respond to climate variability and how they will respond to future climate scenarios. This vast region contains woodlands of phreatophytic species mainly of *Prosopis* spp. and shrublands of several drought-resistant shrubs and small trees (Rundel, 1981; Arroyo et al., 1988; Gajardo, 1994; Armesto et al., 2007; Rundel et al., 2007). The potential of these woody species for dendrochronological studies and climatic reconstruction remains unknown and it has been identified as a high research priority (Lara et al., 2005).

In this work we assess the climate signals in the tree-rings of three high-elevation woody species growing in the semiarid Andes of north-central Chile between 29°45′ and 30°59′S, a well-known ENSO-sensitive region at the southern boundary of the Atacama Desert. This semiarid region represents a steep climatic and vegetation transition between the Atacama Desert, north of 28°S, and the Mediterranean-type ecosystems south of ~30°S. These semiarid ecosystems, constrained by a strong climate seasonality imposed by the Mediterranean regime, occupy a narrow band between ~27° and 32°S locally known as *Norte chico* and are highly sensitive to El Niño-Southern Oscillation variability (Holmgren et al., 2001, 2006).

The main goals of this paper are 1) to analyze the responses of the radial growth of three high-elevation species to precipitation and temperature over the entire semiarid region between 27° and 33°S, and 2) to assess the influences of the El Niño-Southern Oscillation (ENSO) and the low frequency ENSO-like mode of the Pacific Decadal Oscillation (PDO) on regional climate and tree growth variability over most of the last century.
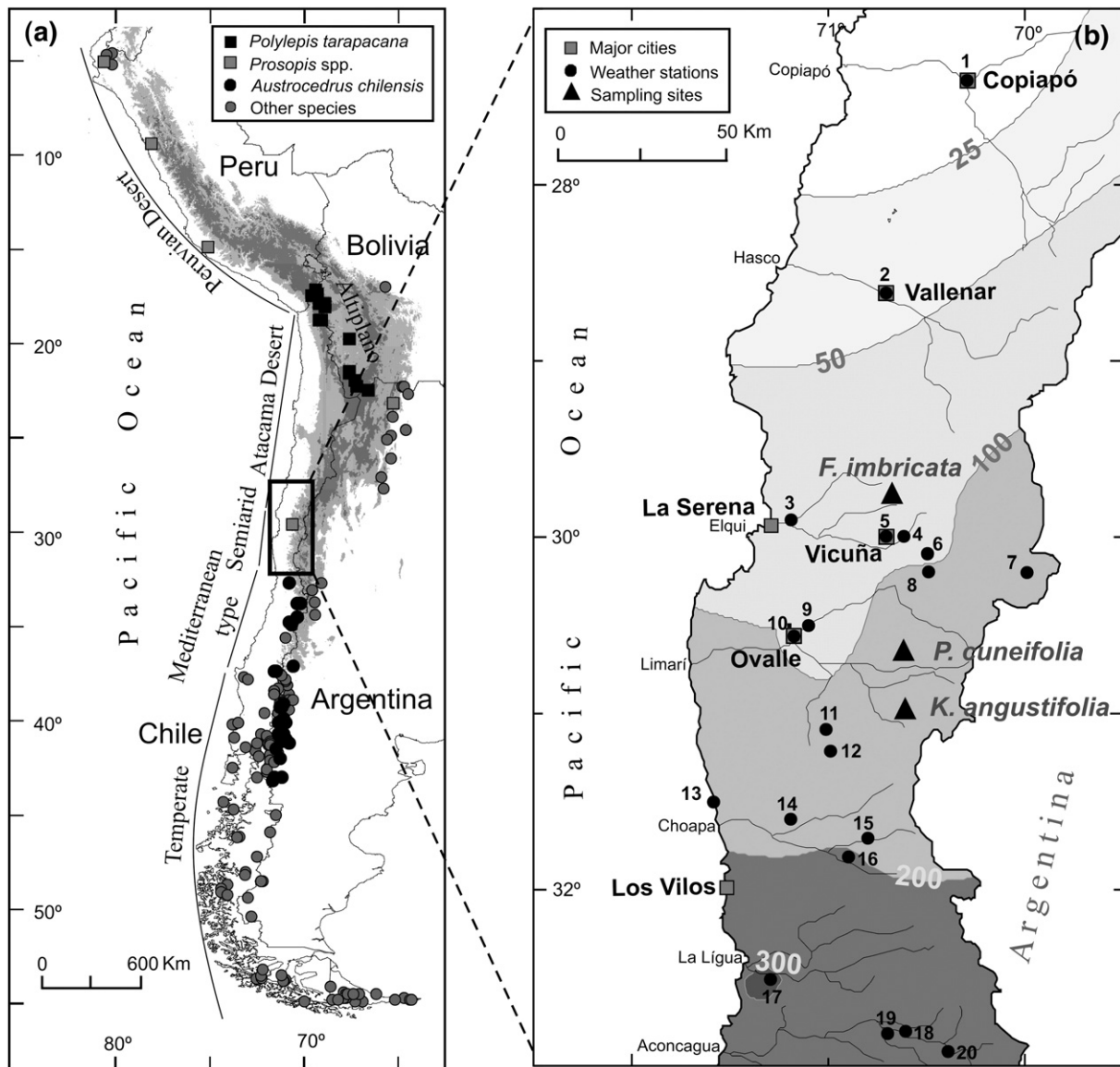
Fig. 1. (a) Map showing the topography and current South American dendrochronological network along the Andes together with the major biogeographic zones through the west coast of South America. The light and dark gray shading indicates elevations above 2000 and 4000 m, respectively. The chronology locations were obtained from the International Tree-Ring Data Bank (http://www.ncdc.noaa.gov/paleo/treering.html) and a literature survey. (b) North-to-south precipitation gradient and location of the tree-ring sites and meteorological stations (see codes in Table 2) in the semiarid region of north-central Chile. The isohyets (mm year^{-1}) are based on the common period 1964–1990 and were calculated using the kriging interpolation method. The main cities and rivers along the region are also indicated.

2. Study area

The semiarid region of north-central Chile (~32°–27°S) represents a steep climatic and vegetation gradient between the Mediterranean-type climate region in central Chile and the hyper-arid Atacama Desert to the north. The regional landscape is characterized by a system of transverse fluvial valleys running east–west from the Andes to the Pacific. Our sampling area is located in the dry Andean foothills of the Elqui and Limarí valleys from 2000 to 2500 m elevation, in the central part of the semiarid region between 29°44′ and 30°59′S (Fig. 1).

2.1. Climate

The semiarid region is located at the northernmost limit of the influence of the Southern Hemisphere westerly winds and their associated fronts that bring winter rainfall as far north as 27°S (Van Husen, 1967; Miller, 1976; Vuille and Amman, 1997). Most of the region is under the persistent influence of the southeastern Pacific subtropical anticyclone that effectively blocks the westerly flow at low levels of the atmosphere contributing to the arid conditions that characterize the Atacama Desert north of 27°S (Miller, 1976; Aceituno et al., 1993). At these latitudes the Andean Cordillera reaches an average elevation of 5000 m forming a massive physical barrier that isolates the west coast from the easterly flow of warm and moist air that brings summer rainfall to the slopes east of the continental divide (Montecinos and Aceituno, 2003; see Fig. 1a). Due to the influence of the subtropical anticyclone and the blocking effect of the Andes, the regional climate is characterized by a Mediterranean-type rainfall regime with a dry period lasting for 9 months (Van Husen, 1967; Miller, 1976). Annual precipitation increases from 25 mm to 200 mm at lowlands between 28° and 32°S and can reach 300 mm at high elevations (>3000 m) in the Andes where it falls almost entirely as snow due to lower temperatures (Almeyda and Sáez, 1958; Miller, 1976). More than ~90% of the annual precipitation falls during the cooler winter months between May and August (Fig. 4), when the subtropical anticyclone and the midlatitude westerlies are at their northernmost annual position ca. 28°S and the occasional fronts can reach the region. On average, about 90% of the total precipitation is associated with the extratropical wave activity in the westerlies, and the remaining 10% is linked with isolated cutoff cyclones (Montecinos and Aceituno, 2003), which produce strong windstorms and heavy precipitation and snowfall at higher elevations of the Andes (Vuille and Amman, 1997; Garreaud and Aceituno, 2007). The intermontane lowlands and lower Andean foothills far from the influence of coastal fog and marine moisture are very dry. In contrast to precipitation, temperatures are remarkably homogeneous and with little seasonal amplitude due to the strong oceanic influence (Miller, 1976). The mean annual temperature in the study area fluctuates around 25 °C, and the mean temperature of the warmest (January) and coolest (July) month ranges from 28 to 30 °C and from 22 to 25 °C, respectively (Almeyda and Sáez, 1958). The sea surface temperature (SST) in the tropical Pacific plays a predominant role in the climate variability of central Chile (30°–35°S; see Garreaud et al., 2009-this issue) through well-known large-scale atmospheric teleconnections (Rutllant and Fuenzalida, 1991; Garreaud and Battisti, 1999). Most of the interannual variability is associated with the El Niño-Southern Oscillation (ENSO), which influences the intensity and latitudinal position of the Southeast Pacific anticyclone

(Pittock, 1980; Aceituno, 1988). Warm El Niño events induce simultaneous higher than average precipitation and temperature, consistent with a relative weak and northward displaced anticyclone connected with an enhanced blocking activity at high latitudes over the south-east Pacific (Aceituno, 1988; Rutllant and Fuenzalida, 1991; Montecinos and Aceituno, 2003). This large-scale atmospheric configuration results in a northward displacement of the midlatitude storm tracks, thus allowing the winter cyclonic storms and related frontal systems to progress into the semiarid region and the southern portion of the Atacama Desert. The opposite atmospheric and climate anomalies tend to occur during the cold La Niña events. The low-frequency climate variability at these latitudes is related to the Pacific Decadal Oscillation (PDO; Garreaud and Battisti, 1999; Villalba et al., 2001; Garreaud et al., 2009-this issue; Villalba et al., in press) and the Interdecadal Pacific Oscillation (IPO; Allan, 2000; Quintana, 2004; Meinke et al., 2005), a quasi-symmetric Pacific-wide manifestation of the PDO that has been described for the North Pacific (Folland et al., 2002). The most prominent low-frequency feature of the rainfall record for north-central Chile (30°–33°S) is a strong decadal fluctuation along with a prevailing negative trend following a period of relatively frequent rainy years at the end of the nineteenth century (Aceituno et al., 1993; Quintana, 2004; see Fig. 3).

2.2. Vegetation and species sampled

Most of the original vegetation in the lowlands and valleys of the semiarid region has been destroyed or highly disturbed by human activities since the 1600s. These disturbances include clearing for irrigated agriculture along the main valleys under elevations of 650 m, cutting for fuelwood, goat overgrazing and human-set fires. As a result, most of the woody species of the region now are threatened and have a high conservation priority (Squeo et al., 2001). Consequently, we targeted high elevation sites for sampling of tree rings in order to avoid the effects of human disturbances on tree growth and to maximize the climatic signal.

The vegetation varies dramatically across the study area, following the regional rainfall gradients and local topography. The north-to-south increase in precipitation is paralleled by a progressive increase in plant cover and abundance of sclerophyllous species typical of central Chile. The dry intermontane slopes at mid-elevations (1000–2000 m) of the Andes are dominated by sparse shrublands of drought-deciduous species such as *Proustia cuneifolia*, *Proustia ilicifolia*, and occasionally by *Trevoa quinquenervia* in the Limarí valley. In the driest locations and xeric north-facing slopes these shrublands are mixed with the columnar cacti *Trichocereus chilensis* and *Trichocereus coquimbana*. At higher elevations (2000–2800 m) montane communities dominated by the evergreen shrub *Fabiana imbricata* and hygrophilous small trees of the genus *Escallonia* are found in moist environments along small ravines and springs. The adjacent dry slopes are dominated by multi stemmed shrubs of *P. cuneifolia*, *Adesmia hystrix*, and *Ephedra breana*. In the Limarí valley, the northernmost populations of *Kageneckia angustifolia* (Squeo et al., 2001) form a discontinuous tree-line between 1800 and 2300 m. This species is a small evergreen tree that generally forms the scattered tree-line along the Mediterranean Andes of central Chile between 30°22′ and 35°S (Table 1).

In this study we sampled three high elevation species in the Elqui and Limarí valleys that have not been previously used in dendrochronology

Table 1
Sampled species and sites.

Sampled species	Growth form	Family	Leaf phenology	Geographic range (Lat. S)	Sampling site		
					Location	Lat. (S), Lon. (W)	Elevation (m)
Kageneckia angustifolia D. Don	Tree	Rosaceae	Evergreen	30°22′–35°05′	Limarí valley	30ª59′, 70°38′	2100
Proustia cuneifolia D. Don	Tall shrub	Compositae	Summer-deciduous	19°32′–37°41′	Limarí valley	30°42′, 70°40′	1900
Fabiana imbricata Ruiz et Pav.	Shrub	Solanaceae	Evergreen	28°03′–39°38′	Elqui valley	29°44′, 70°37′	2550

(Table 1, Fig. 1b). In the Limarí Valley we sampled an open shrubland of *P. cuneifolia* (Compositae) with old individuals at 1900 m and a tree-line of *K. angustifolia* (Rosaceae) between 2100 and 2200 m (Table 1). In the Elqui Valley we collected samples from a shrubland of *F. imbricata* (Solanaceae) in a small ravine at 2550 m in the upper part of the Quebrada Marqueza at 29°44′S. This is the highest and northernmost sampling site (Fig. 1) and represents the northern margin of the latitudinal distribution of this species (Table 1).

3. Methods

3.1. Sample processing and tree-ring chronology development

Cross-sections and wedges from dead and living individuals were collected using a chainsaw. We preferred cross-sections and wedges instead of increment cores to increase the size of the observation area and the number of radii that could be analyzed for each particular tree. This was in order to improve the discernment of tree-rings and to reduce problems with locally missing rings due to the stem irregularity and cambial death probably associated with severe droughts. We also sampled young branches to overcome crossdating problems due to a severe growth suppression induced by a short drought during the 1990s in most of the stem samples of *Kageneckia*. We used standard dendrochronological procedures for processing the samples and to develop tree-ring width chronologies (Stokes and Smiley, 1968; Fritts 1976). After mounting, sanding, and visual crossdating under a stereomicroscope, ring widths were measured to the nearest 0.001 mm with a stage micrometer. For dating purposes we adopted Schulman's (1956) convention for the Southern Hemisphere and assigned dates of annual rings to the year in which radial growth started (i.e. winter–spring). Bar plots representing graphically the standardized year-to-year tree-ring width variability (Holmes, 1983) were used for easy intercomparison between samples to detect the growth pattern at each site and to overcome crossdating problems due to suppressed, missing or discontinuous growth rings.

Visual crossdating and measurements were checked using the program COFECHA (Holmes, 1983), which computes a series of correlation coefficients between overlapping segments of each individual tree-ring series against the mean site series to detect absent or false rings. Once the tree-ring series were correctly dated, ring-width data

were detrended, standardized, and combined into a mean site chronology using the program ARSTAN40c (Cook and Krusic, 2006), which produces standard and residual chronologies (Cook, 1985). The standard chronology is simply the average (robust mean function) of all the standardized tree-ring series while the residual chronology is the average of the residuals series resulting from autoregressive modeling of each individual tree-ring series (Cook, 1985). The use of residual (i.e. prewhitened) chronologies generally is necessary in tree-ring studies. By removing the serial persistence from tree-ring series, some statistical assumptions are satisfied and the statistical significance can be properly determined in parametric correlation analysis (e.g., correlation with climate variables). To remove non-climatic biological age-related growth trends in the tree-ring widths and to maximize the common signal (Fritts, 1976), the raw individual series were detrended and standardized by dividing the measured values by the value of a negative exponential function or linear regression with negative slope (Cook and Kairiukstis, 1990). We used this conservative detrending to preserve as much as possible the low-frequency variability in our short tree-ring series while maximizing the climate signal. Using this conservative detrending, the lowest frequency of climate information that can be realistically recovered is $3/n$ cycles per year (Cook et al., 1995), where $n =$ the mean sample length. Therefore, with mean site sample lengths ranging between 49 and 85 years (Table 4), our chronologies can properly represent variability at interdecadal (~16–30 years) or higher-frequency time scales.

The quality and signal strength of the chronologies through time were assessed using the Expressed Population Signal (EPS) statistic (Wigley et al., 1984) via a moving window analysis with 30-year running windows with an overlap of 15 years. EPS is a measure of the agreement between the mean chronology and the population, represented by a hypothetical chronology that has been infinitely replicated from the individual series comprising the chronology (Briffa, 1995). We utilized the commonly applied 0.85 threshold to denote reasonable signal strength (Wigley et al., 1984).

3.2. Climate data and regional series

Monthly precipitation data for the semiarid region between ~27° and 33°S (Copiapó–Los Andes) were compiled from all the available stations at low and high elevations covering the 1964–1990 common period and with <30% missing data (Table 2, Fig. 1). These records

Table 2
Meteorological stations used in this study and correlation between winter (June–August) precipitation and the tree-ring chronologies over the period 1964–1990.

ID	Station	Latitude S	Longitude W	Period	Elevation (m)	Source	Annual average (mm)	Correlation with winter precipitation		
								Kageneckia	Proustia	Fabiana
1	Copiapó	27°22′	70°19′	1951–1990	370	**	12.2	0.12	0.44*	0.45*
2	Vallenar	28°34′	70°43′	1951–1990	650	**	38.0	0.12	0.44*	0.45*
3	La Serena	29°54′	71°15′	1869–2000	50	DMC	73.7	0.43*	0.57*	0.62*
4	Rivadavia	29°58′	70°36′	1916–2000	820	DGA	94.8	0.53*	0.54*	0.64*
5	Vicuña	30°02′	70°35′	1930–2000	610	DMC	89.0	0.42*	0.56*	0.67*
6	Monte Grande	30°05′	70°29′	1964–2003	1115	DGA	69.5	0.61*	0.56*	0.55*
7	La Laguna	30°11′	70°02′	1964–2003	3100	DGA	180.1	0.74*	0.52*	0.35
8	Los Nichos	30°12′	70°30′	1961–2000	1310	DMC	125.1	0.61*	0.62*	0.63*
9	Emb. Recoleta	30°30′	71°06′	1959–2000	400	DGA	78.7	0.56*	0.60*	0.56*
10	Ovalle	30°36′	71°12′	1912–2000	220	DGA	99.5	0.37	0.56*	0.42*
11	Cogotí	31°06′	71°00′	1953–2000	650	DGA	109.2	0.26	0.42*	0.30*
12	Combarbalá	31°11′	71°02′	1930–2000	900	DMC	203.0	0.58*	0.67*	0.58*
13	Puerto Oscuro	31°27′	71°36′	1930–2000	10	DMC	171.4	0.45*	0.59*	0.60*
14	Illapel	31°36′	71°11′	1930–2000	310	DMC	156.5	0.54*	0.62*	0.53*
15	San Agustín	31°42′	70°48′	1931–2000	1280	DGA	149.0	0.23	0.36	0.03
16	Salamanca	31°48′	70°55′	1961–2000	570	DMC	217.7	0.46*	0.67*	0.50*
17	La Ligua	32°27′	71°16′	1930–2000	60	DMC	310.7	0.56*	0.62*	0.47*
18	San Felipe	32°45′	70°44′	1930–2000	630	DMC	207.6	0.53*	0.65*	0.55*
19	Los Andes	32°50′	70°37′	1907–2000	815	DMC	271.1	0.64*	0.61*	0.48*
20	Riecillos	32°54′	70°24′	1930–2000	1290	DGA	253.3	0.35	0.56*	0.58*

**: Mathias Vuille (pers. comm.), Climate System Research, University of Massachusetts, USA.
The asterisk symbol "*" denote significant ($p < 0.05$) correlations. The spatial location of the stations is also indicated in the Fig. 1b.

were primarily obtained from the Dirección Meteorológica de Chile (DMC) and Dirección General de Aguas (DGA). Most of this dataset has been used in a regional analysis of climate trends and the series have been corrected for inhomogeneities (Quintana, 2004), thus we did not perform homogeneity tests. Missing data for a specific station were filled using as reference the nearest highly correlated station. Missing values were estimated as the product of the monthly value in the reference station and the ratio between the long-term mean monthly averages of the candidate and the reference series for that month (Alexandersson, 1986; Štěpánek, 2005). Using techniques outlined in Jones and Hulme (1996), the data were averaged to formulate regional monthly series of precipitation with respect to the common period 1964–1990 and based on twenty stations (Table 2). This regionalization of the precipitation data helped to optimize the common signal and maximized the final length (1869–2000) of the precipitation record, although the anomalously wet period before 1907 is covered only by the La Serena weather station (Fig. 3b, Table 2). For a regional record of temperature, we used monthly $5° \times 5°$ gridded anomalies series of mean land surface air temperature from the CRUTEM3 dataset (Brohan et al., 2006) for north-central (25°–30°S, 70°–75°W) and central (30°–35°S, 70°–75°W) Chile. Comparative visual analysis showed minor differences between the monthly time series of these two grid boxes due to the very homogeneous temperature regime along the coast. Therefore, these data were averaged together to obtain a regional record of mean monthly air temperature from 1861 to 2004 (Fig. 3a).

3.3. Influences of regional climate on tree growth

To assess the relationships between climate and tree growth, we correlated the residual tree-ring chronologies with the individual series of regional monthly precipitation totals and monthly mean air temperature for the current growth year from January to December. Prior to correlation analysis all the climate series were prewhitened using an autoregressive model (AR) with the AR(p) order selected by the first minimum of the Akaike Information Criteria (AIC; Akaike, 1974). To identify the spatial patterns and subregional responses of tree growth to precipitation each residual tree-ring chronology was correlated with the observed winter (June–August) precipitation.

3.4. Oscillation modes

Tree-rings and climate records, as many other geophysical time series, simultaneously integrate trends, oscillatory components, and noise (Ghil et al., 2002). The spectral analysis and decomposition of these univariate time series enables the separation of signals represented by trends, quasi-periodic and other oscillatory components from the variations representing noise. We used Continuous Wavelet Transform analysis (WT; Torrence and Compo, 1998; Grinsted et al., 2004) to identify the dominant oscillatory modes of variability in tree growth and regional climate series at different time scales. The WT analysis is a powerful tool for the identification of nonstationary signals because it decomposes the time series into frequency components in the time–frequency space and then characterizes the variance in each component, enabling the identification of the

dominant modes of variability and how those modes vary through time (Torrence and Compo, 1998; Jevrejeva et al., 2003). The statistical significance was estimated against a red noise model at the 95% confidence level (Torrence and Compo, 1998). The wavelet analysis was complemented with Maximum Entropy Spectral Analysis (MESA; Ghil et al., 2002; Štěpánek, 2005) to accurately obtain the periods of the significant spectral peaks observed in the wavelets. The MESA spectrum was estimated from a number of lags of the autocorrelation function corresponding to 25% of the series length and the number of calculated frequencies was also fixed to 25% of the series length. These settings were found to produce coherent results with wavelet analysis.

3.5. Influences of ENSO and PDO on regional climate and tree growth

The regional climate series and the tree-ring chronologies were compared with indices of ENSO and PDO (see Table 3) in both time and frequency domains. Linear correlations were calculated between the residual tree-ring chronologies and monthly sea surface temperature (SST) of the Niño 3.4 region and PDO index over the current growth year from January to December. The monthly time series of these indices are strongly autocorrelated and thus we used prewhitening prior to correlation analysis. In the case of PDO, prewhitening can remove an important fraction of the low frequency signal under study. Therefore, in order to avoid this shortcoming we also correlated the standard tree-ring chronologies and the raw monthly PDO index, adjusting for the loss of degrees of freedom due to serial persistence in the data (Dawdy and Matalas, 1964). However, no differences in the pattern of correlations were found using this approach and thus we only show the results from the prewhitened series.

The El Niño and La Niña events during the period 1871–2000 were objectively identified using the Trenberth (1997) criteria. Thus, we defined an El Niño (La Niña) event if the 5-month running mean of the SST anomalies in the Niño 3.4 region exceeded $+0.4$ (-0.4) °C within the season from March to September. We used this temporal window because it is the period when the tropical Pacific SSTs influence the precipitation regime and hence tree growth in the semiarid region. When El Niño and La Niña occurred simultaneously in the same year (15 cases), only the most persistent event was assigned to this year. Superposed epoch analysis (SEA; Holmes and Swetnam, 1994) was applied to these events of El Niño and La Niña to examine the mean pattern of anomalies in annual precipitation, mean temperature during the rainy season (April–September), and residual tree-ring chronologies. A 4-year interval (2 years previous and 2 years after each event) was used as the time window. In this analysis, windows for each event are superimposed and averaged, and the mean pattern emerging is examined for statistical significance through 1000 random Monte Carlo simulations that provide 95% bootstrap confidence intervals (Holmes and Swetnam, 1994).

Finally, we used Cross Wavelet Transform analysis (XWT; Grinsted et al., 2004) to assess the strength, significance and relative phase of any common oscillation mode between these climate forcings and regional climate and tree growth. This cross-spectral technique allowed us to test the physical linkages (Jevrejeva et al., 2003; Grinsted et al., 2004) between the climate forcings and the regional climate and tree growth time series by identifying

Table 3
Indices used to evaluate the influences of ENSO and PDO on climate and tree growth.

| Climate index description	Period	Data source	Reference
Niño 3.4 SST Mean monthly SST anomalies for the Niño 3.4 Region, east central Tropical Pacific (5°N–5°S, 170–120°W)	1871–2004	Dennis Shea (pers. comm.), NCAR, Boulder, CO, USA.	Hurrel et al. (2008)
Pacific Decadal Oscillation (PDO) Leading Principal Component of monthly SST anomalies in the north Pacific Ocean, poleward of 20°N	1900–2006	JISAO http://jisao.washington.edu/pdo/PDO.latest	Mantua et al. (1997)
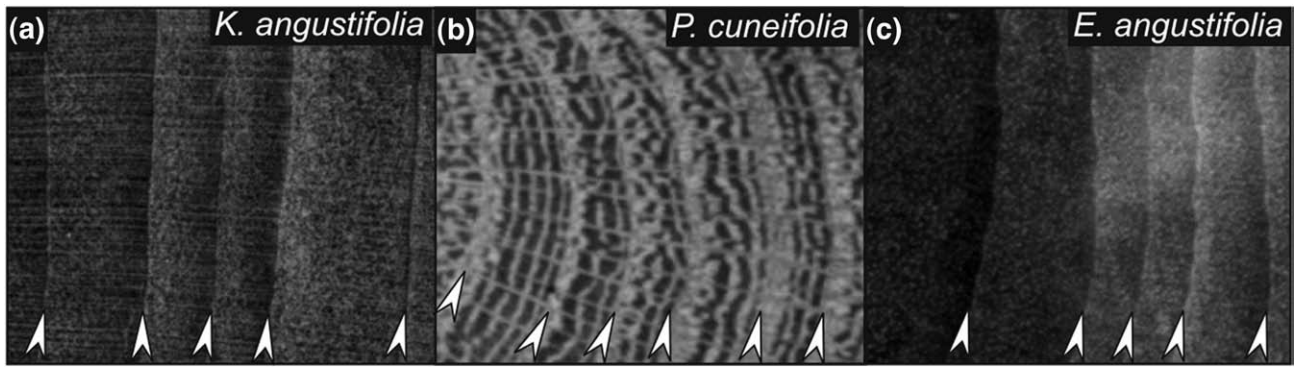
Fig. 2. Cross-sections showing the tree-ring morphology of (a) *K. angustifolia*, (b) *P. cuneifolia*, and (c) *E. angustifolia*. The white arrows indicate the ring boundaries.

regions in the time–frequency space where the series show high and coherent common power, consistent with the physical mechanisms driving the climate variability in the region. The statistical significance was assessed against a red noise background by means of

Monte Carlo methods (Grinsted et al., 2004). Because of the summer-dormancy in cambial activity induced by the extended period of drought, the seasonal response of tree growth in our sites is mainly restricted to the rainy season (April–September; see Fig. 4); thus we
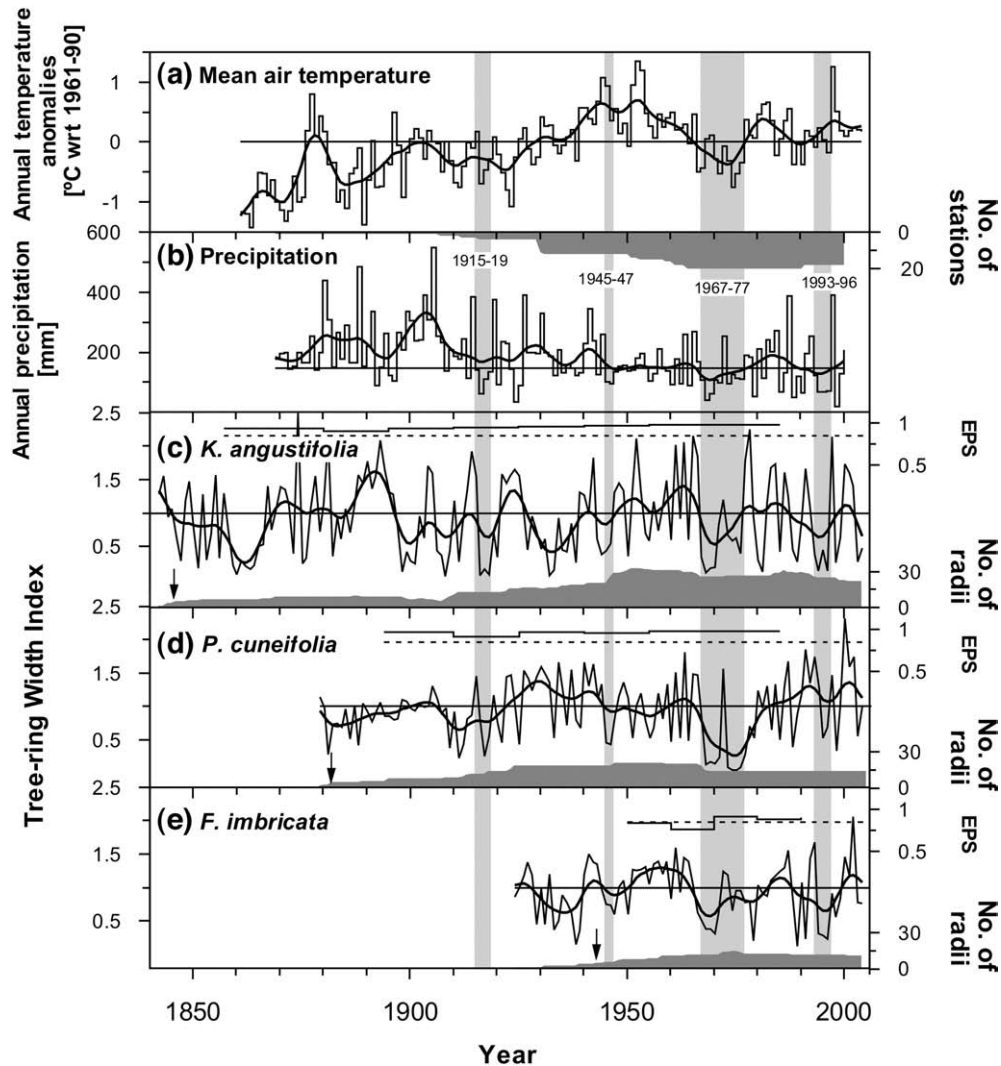

Fig. 3. (a) Regional series of mean air temperature based on the 5°×5° grid cells of the CRUTEM3 dataset for north-central (25°–30°S, 70°–75°W) and central (30°–35°S, 70°–75°W) Chile. (b) Regional precipitation along the semiarid region between 27° and 33°S. This series resulted from the back transformation (see Jones and Hulme, 1996) of the precipitation anomalies respect to the common period 1964–1990. The number of stations included in the record through the time is indicated in the upper part of the panel. (c–d) Standard tree-ring width chronologies of *K. angustifolia*, *P. cuneifolia*, and *F. imbricata*. The running Expressed Population Signal (EPS) statistic calculated for 30-year windows and sample depth through time are shown for each chronology. The horizontal dotted lines denote the 0.85 EPS threshold. The vertical arrow indicates when the number of radii available back in time falls below 5. To emphasize the low-frequency variation each time series is also shown in a smoothed version (bold line) using a 12-year cubic spline. The vertical gray bands indicate the major multi-year droughts through the region.

Table 4
Sample sizes and descriptive statistics for the three standard tree-ring width chronologies.

Species	Period	No. of years	No. of trees (radii)	Series length in years (mean, range)	Mean tree-ring width (mm)	Mean sensitivity[a]	Mean Rbar[b]	Variance in the first eigenvector (%)
Kageneckia angustifolia	1842–2004	163	31 (47)	64, 20–124	1.16	0.70	0.49	57.2
Proustia cuneifolia	1879–2004	126	11 (21)	85, 35–127	0.89	0.51	0.57	71.7
Fabiana imbricate	1924–2004	81	10 (15)	49, 24–81	1.04	0.45	0.38	46.6

[a]Mean sensitivity is a measure of the relative changes in ring width variations from year to year (Fritts, 1976).
[b]RBAR is the mean correlation coefficient between all the possible combinations of tree-ring series (radii) in the chronology (Briffa, 1995).
[c]Variance in the first eigenvector is the percentage of common variance among tree-ring series explained by the first principal component.

averaged the mean air temperature, and the Niño 3.4 SST and PDO index over this period to produce a representative time series for comparison with tree growth. These seasonal series, together with the annual precipitation and the two longest standard tree-ring chronologies (*K. angustifolia* and *P. cuneifolia*), were used as input series in the XWT analysis.

4. Results

4.1. Tree-ring chronologies and regional climate series

The tree-rings of the three species are well-demarcated and can be easily identified (Fig. 2). The *K. angustifolia* and *F. imbricata* tree-rings can be discriminated by a combination of diffuse to semi-ring porosity with a band of radially flattened fibers in the latewood that marks the ring boundary (Fig. 2a, c). The *P. cuneifolia* growth rings are characterized by a pattern of tangential parenchyma bands in the latewood and ring to semi-ring porosity (Fig. 2b), and the boundaries can be unequivocally identified by a band of marginal parenchyma. Over 90% of the samples of the three selected species collected at each site were successfully crossdated. Crossdating was especially difficult due to the presence of partially absent rings in most of the samples during periods of extremely slow growth associated with regional droughts in 1915–19, 1945–47, 1967–77, and 1993–96 (Fig. 3). Sample sizes vary from a low of 10 individuals and 15 radii for *Fabiana imbricata* to a maximum of 31 trees and 47 radii for *K. angustifolia* (Table 4). The chronology lengths closely match the species lifespans and range between 81 years for *F. imbricata* and 126 and 163 years for *Proustia cuneifolia* and *K. angustifolia*, respectively (Table 4). Only the *K. angustifolia* chronology, spanning the interval from 1842 to 2004, surpasses the longest regional climate record starting in 1861 (Table 4, Fig. 3).

All three chronologies have an extremely high year-to-year variability and common signal as indicated by the high values of mean sensitivity (0.45–0.7), Rbar (0.38–0.57), variance in the first eigenvector (46.6–71.7%), and EPS statistics (Table 4; Fig. 3). Mean sensitivity characterizes the year-to-year variability in a chronology and our high values of this statistic reflect an extremely high environmental variability, especially at the xeric tree-line site of *K. angustifolia* (Table 4). The high values of the statistics measuring common variance and signal among trees (Rbar–i.e. mean series intercorrelation–and variance in the first eigenvector) indicate a strong common macroenvironmental influence on tree growth at each site. The strength of this common signal is maintained through time as indicated by high running EPS values above the 0.85 threshold (Fig. 3).

The regional climate over the last century is characterized by a long-term increase in temperature and reduction in precipitation following a prominent wet period at the end of the nineteenth century (Fig. 3a–b). The temperature record also shows the well-known step to increased temperature in 1976, which affected most of the west coast of North and South America (Villalba et al., 2001). Another important feature is a cool period before 1940 followed by a warm period associated with reduced precipitation variability to the early 1960s (Fig. 3a–b). A correlation matrix (Table 5) between the three chronologies and regional temperature and precipitation shows that all the chronologies are significantly ($p < 0.01$) and positively inter-correlated, and also with precipitation. Although not significant, except for *P. cuneifolia*, the chronologies are also positively correlated with annual temperature. The significant correlations among the chronologies indicate the existence of a common pattern of tree growth variability through the region. Interestingly, despite the opposite long-term trends, annual precipitation is highly and positively correlated ($p < 0.01$) with annual temperature during the common period 1924–2000, indicating that these variables varied relatively in-phase through the region over this interval. However, these variables are not correlated ($r = 0.08$, $p > 0.05$) over their entire common period between 1869 and 2000. The high and positive correlations over the period 1924–2000 are explained by the high frequency of ENSO events, which induce anomalies of the same sign in temperature and precipitation (see Fig. 7). As confirmed by the high intercorrelation levels, the tree-ring chronologies as well as the precipitation and temperature series show a coherent common mode of decadal fluctuation superposed to periods of increased and reduced interannual variability (Fig. 3). The chronologies closely follow the interannual and decadal variability in precipitation but do not show any significant long-term trend likely due to the short mean series length (Table 4). In general most of the multi-year droughts are associated with severe growth reductions. The most important synchronic growth reduction in the chronologies occurred during a prolonged drought between 1967 and 1977, interrupted only by a strong wet El Niño event in 1972. The amplitude in the growth of *K. angustifolia* does not quite match the wet period before 1910, although a relative phasing is observed especially in the extremely wet years. The difference in amplitude is likely related to the low number of stations and hence less spatial representation in the early part of the regional precipitation record, especially before 1907 when it is composed only of the La Serena Station (Table 2). In this same period, the chronology of *P. cuneifolia* shows a reduced interannual variability when the individuals included in the chronology were younger than ~20–35 years (Fig. 3d).

Table 5
Correlation coefficients between the residual tree-ring chronologies and regional temperature and precipitation series over the 1924–2000 common period.

| Series	K. angustifolia	P. cuneifolia	F. imbricata	Annual temperature
P. cuneifolia	0.47**			
F. imbricate	0.36**	0.46**		
Annual (Jan–Dec) temperature	0.24	0.29*	0.18	
Annual (Jan–Dec) precipitation	0.44**	0.68**	0.50**	0.47**

* $p < 0.05$, ** $p < 0.01$.

4.2. Influences of regional climate on tree growth

Annual and monthly correlation between the tree-ring chronologies and regional climate (Table 5; Fig. 4) indicate that above-average precipitation and temperature favors tree growth but that precipitation is the dominant climatic signal for all three species. Annual correlations show that at our sampling sites regional precipitation alone explains between 20 and 46% of the total variance in tree growth, whereas temperature can explain 8% at most (Table 5). Monthly correlations (Fig. 4) indicate that the tree-ring chronologies are significantly and highly correlated ($p < 0.05$) with precipitation from July through September (winter and early-spring), the period when the maximum cambial activity occurs in the summer-deciduous *P. cuneifolia* (Aljaro et al., 1972) and just prior to the growing season (typically spring–summer) of *K. angustifolia* (Piper et al., 2006) and probably also *F. imbricata*. The responses of tree growth to regional temperature are also positive throughout the year but vary greatly between species in both magnitude and timing (Fig. 4). The growth of *K. angustifolia* at the tree-line site shows a positive significant response to temperature between August and October (winter–spring), whereas the highest response to temperature of *P. cuneifolia*

and *F. imbricata* occurs in April (mid autumn), at the beginning of the rainy season. In addition, although marginally significant the growth of *P. cuneifolia* is also correlated with June and August temperature. In summary, wet and warm conditions during the rainy season significantly favor the radial growth of these high elevation species but winter precipitation is the main climate control.

The spatial patterns of correlation between the tree-ring chronologies and winter (June–August) precipitation over the common period 1964–1990 are characterized by an abrupt break at ~30°S (Fig. 5; Table 2), with the highest correlations occurring south of 30°S where the annual precipitation is above 70 mm (Table 2). Only the two northernmost chronologies (*F. imbricata* and *P. cuneifolia*) are significantly correlated with precipitation stations north of 30°S. In the region south of 30°S there is not a clear common gradient in correlations and in general the chronologies have the highest correlations ($r = \sim 0.6$–0.74) with the nearest precipitation stations, usually located in the same valley. The chronologies of *F. imbricata* and *P. cuneifolia* have more homogeneous correlations through the region than the chronology of *K. angustifolia*, explaining their highest correlations with the regional record of precipitation (Table 2). In contrast, the growth of *K. angustifolia* at the tree-line site has a more
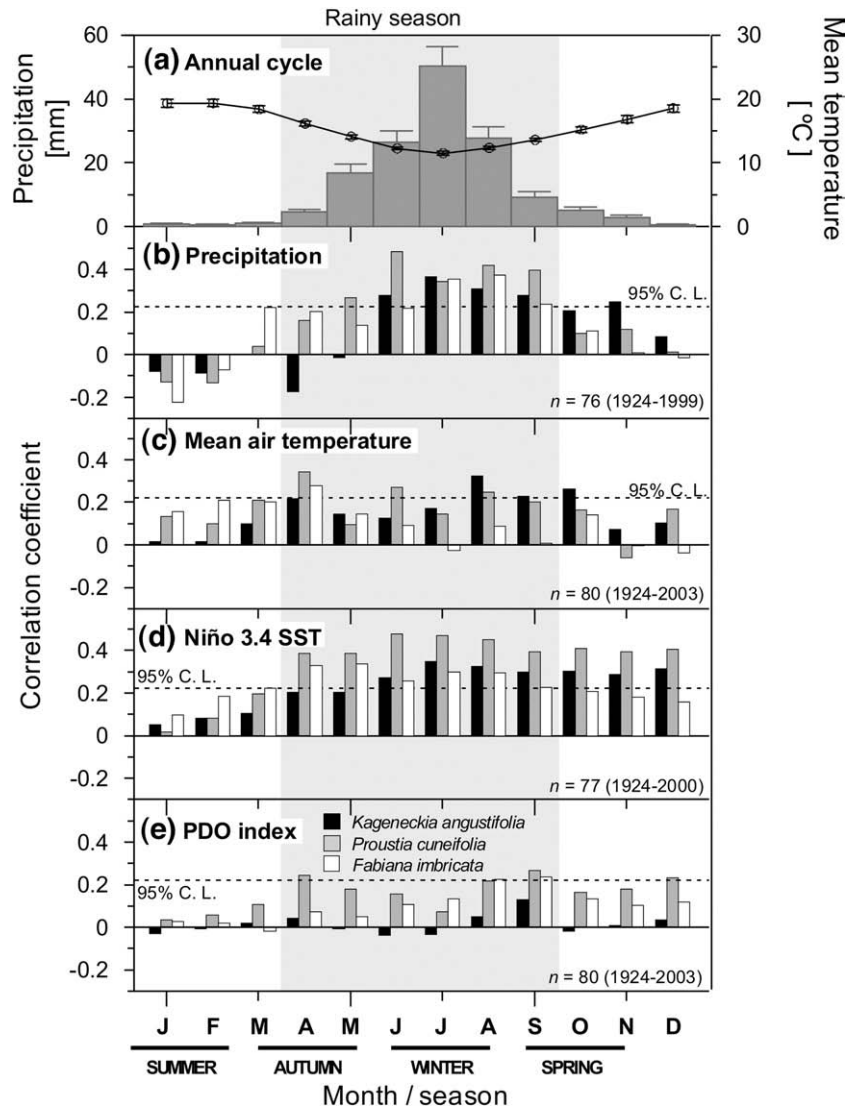
Fig. 4. (a) Annual climate cycle in the semiarid region. (b–e) Monthly correlations between the residual tree-ring chronologies and regional precipitation and temperature, and the prewhitened Niño 3.4 SST anomalies and PDO time series. Positive correlation indicates that above-average tree growth is associated with above-average values of the target climatic variable. The common period used for correlation analysis is indicated in each panel.
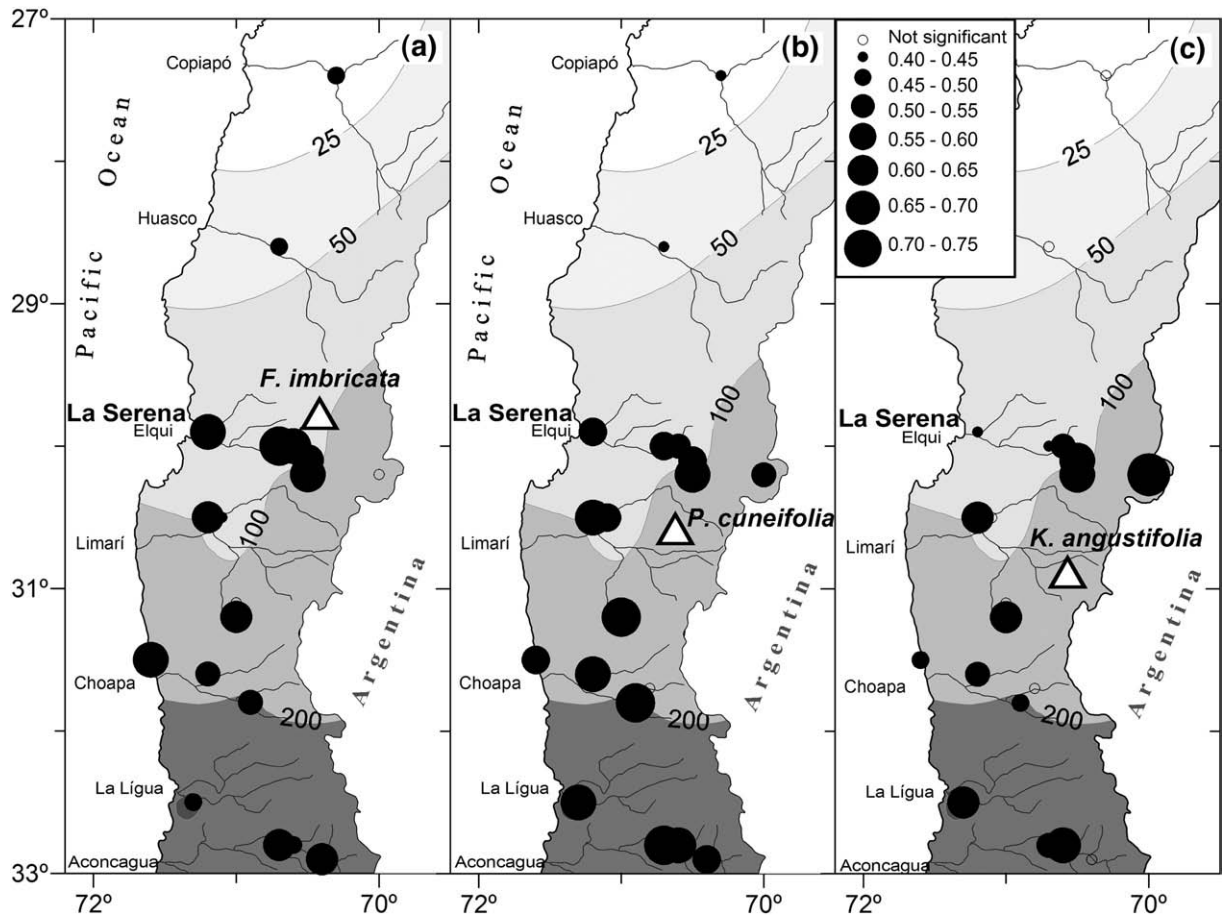
Fig. 5. Spatial correlation patterns between winter (June–August) precipitation at each station and the residual tree-ring chronologies of (a) *F. imbricata*, (b) *P. cuneifolia*, and (c) *K. angustifolia* over the period 1964–1990 ($n = 37$ years). The precipitation gradient and the major rivers are shown as background.

local response and is best correlated with the few stations located at mid and high elevations (>900 m; Table 2). Indeed, the best correlation ($r = 0.74$) occurs with the highest station located at 3100 m in the upper part of the Elqui valley (Fig. 5c). Interestingly, among the species the *K. angustifolia* growth has the lowest correlation with the longest record of precipitation at La Serena station (Fig. 5).

4.3. Oscillation modes in the regional climate and tree growth variability

The wavelet power spectra of the climate series and the standard tree-ring chronologies (Fig. 6) show significant and nonstationary variability from interannual (2–8 years) to multidecadal timescales (>30 years). The rainy season (April–September) temperature and annual precipitation series have remarkably similar spectral signatures with a particular and robust bidecadal oscillatory signal (~21-year period) coupled with high decadal and interannual variability between ~1870 and 1920, followed by a relatively quiescent period interrupted by significant interannual variability in the 1950s and 1980–1990s (Fig. 6b–c). Interestingly, the coupling of this bidecadal signal with high interannual variability coincides with the anomalous wet period observed in the regional record of precipitation (Fig. 3b), suggesting that this particular period resulted from an unusual interaction of low and high frequency signals. Precipitation shows no lower frequency signal over the record whereas temperature has a significant 44-year multidecadal trend (Fig. 6b). On the other hand, the wavelet power spectra of the tree-ring chronologies show increased interannual variability since the 1970s and more persistent

interdecadal and multidecadal variability through time, although barely significant (Fig. 6d–f). MESA detects significant spectral peaks at decadal and interdecadal domains from 8 to 12-year and from 20 to 24-year periods, respectively (Fig. 6d–f). The wavelet spectrum of *K. angustifolia* (Fig. 6d) shows high but insignificant power at interdecadal and multidecadal domains; MESA identifies significant spectral peaks at 20, 32 and 40-year periods, which closely match those of precipitation and temperature. In particular, the presence of shared multidecadal peaks (~32 and 40-year period) with temperature agrees with the statistically significant response of this species to winter–spring temperature (Fig. 4c), thus indicating a multidecadal influence of temperature on tree growth. A similar and coherent pattern of temperature-modulated multidecadal variability with a ~37-year period is apparent in the chronology of *P. cuneifolia* (Fig. 6e). The chronology of *F. imbricata* has very strong interannual variability but restricted only to the 1980–1990 decades and despite its short length also captures significant low frequency at decadal and interdecadal domains between 8 and 24 years (Fig. 6f).

4.3.1. Influences of large-scale climate modes

The comparison between the tree-ring chronologies and the Niño 3.4 SST and PDO index (Fig. 4d–e) shows a strong response of tree growth to tropical Pacific conditions contrasting with a poor relationship with the PDO in the three sampled species. The three chronologies are significantly and positively correlated with the Niño 3.4 SST index from late autumn to summer (April–December), although the chronology of *F. imbricata* losses significance in the early spring (Fig. 4). In contrast, the PDO index is poorly correlated with tree
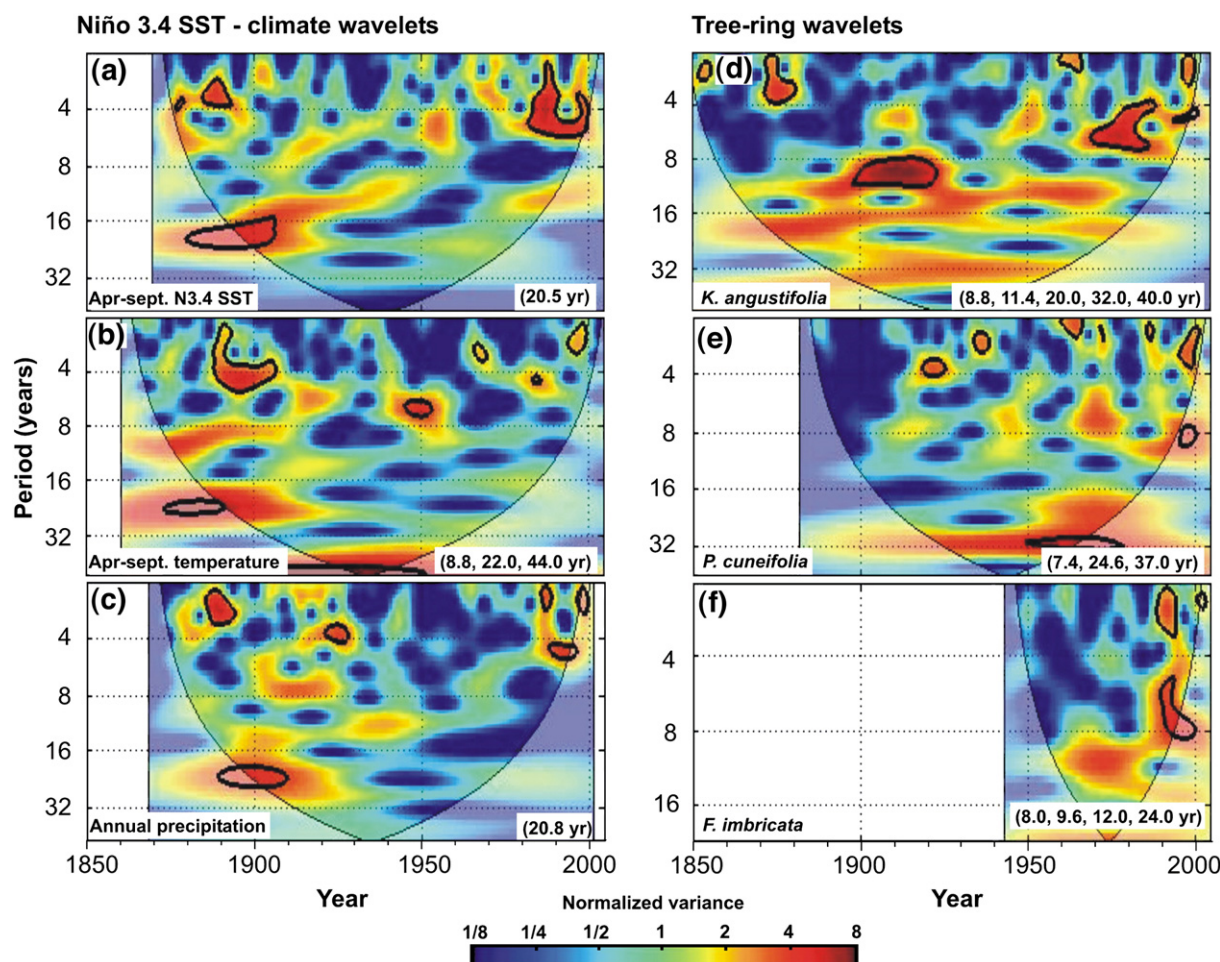
Fig. 6. Continuous wavelet power spectrum of the seasonalized N3.4 SST (a), (b–c) regional climate series, and (d–f) standard tree-ring chronologies. The thick black contour designates the 5% significance level against red noise and the cone of influence (COI), where edge effects might distort the picture, is shown as a lighter shade. In each wavelet panel the >8 years significant peaks (*p*<0.05) obtained with Maximum Entropy Spectral Analysis are indicated in parenthesis.

growth and only the chronologies of *P. cuneifolia* and *F. imbricata* have common and significant positive correlations at the end of the rainy season during August–September (Fig. 4d–e).

El Niño events are recorded in general as positive departures in tree growth (Fig. 7c–d) due to increased precipitation and temperature induced by these events (Fig. 7a–b). Conversely, La Niña events are associated with negative departures in tree growth (Fig. 7c–d) as a consequence of cold-dry conditions (Fig. 7a–b). The climate anomalies induced by both El Niño and La Niña conditions (Fig. 7a–b) are all significant (*p*<0.05), whereas the tree growth anomalies are at the best marginally significant (Fig. 7c–e). This indicates a great inter-event variability in the responses of tree growth to the ENSO-induced climate anomalies and it is probably related to local site conditions.

The XWT analysis (Fig. 8a–b) reveals consistent and significant in-phase covariance between the Niño 3.4 SST and precipitation, temperature and tree growth within the classical ENSO bandwidth from 2 to 7 years and also at a bidecadal scale, confirming the results found in the correlation analysis (Fig. 4d). Indeed, the power spectra of the temperature and precipitation series (Fig. 6b–c) have the spectral fingerprint of ENSO at these timescales (Fig. 6a). These results reveal that the bidecadal signal in the climate of the semiarid region (Fig. 6b–c) during the extremely wet period between 1870 and 1920 (Fig. 3b) is linked to a dominance of warm conditions in the tropical Pacific during this period at both interannual and bidecadal time-scales. Similar to the climate series, the XWT between the Niño 3.4 SST and the chronology of *K. angustifolia* (Fig. 8c) shows that significant tree-ring width signals at interannual and interdecadal scales are

linked to conditions in the tropical Pacific. However, there is an antiphase relationship in the bidecadal signal between 1870 and 1920 as opposed to the interannual band, where the two variables vary in-phase (Fig. 8c). At the *K. angustifolia* site we found a fire-scar dated to 1891 in several trees and thus this antiphase relationship could be related to fire disturbance rather than with climate variability. The growth of *P. cuneifolia* covaries significantly and in-phase with the Niño 3.4 SST only within the interannual ENSO bandwidth (Fig. 8d). Nevertheless, there is also a consistent but insignificant in-phase relationship at decadal and interdecadal scales. The XWT between the PDO index and the climate series (Fig. 8e–f) and the tree-ring chronologies (Fig. 8g–h) confirms the poor influence of the PDO in the region. In general, there is significant common power only at the interannual scale but the phase is fairly randomly distributed, suggesting a non coherent relationship. However, there is a consistent but insignificant in-phase relationship with tree growth at the interdecadal scale (Fig. 8g–h). Overall these results indicate that the low frequency variability in both climate and tree growth throughout the region is not related to PDO forcing as measured in the North Pacific.

5. Discussion and conclusions

The arid and semiarid regions spanning the Atacama Desert and north-central Chile are currently a gap in the South American tree-ring network (see Fig. 1a). Only one tree-ring chronology has been published for the region (López et al., 2006) and little is known about
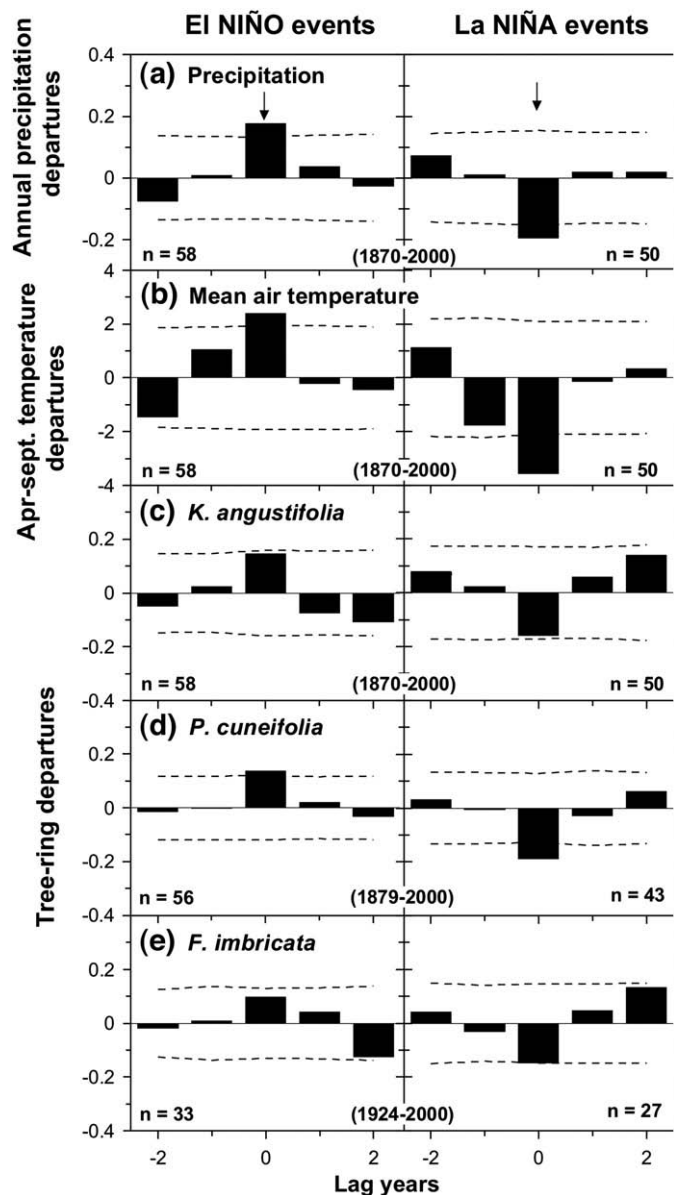
Fig. 7. Departures of (a) annual precipitation, (c) rainy season temperature, and tree-ring index (c–e) for 2 years prior to and 2 years following El Niño and La Niña events (year 0). The dashed horizontal lines represent the 95% confidence levels estimated from 1000 Monte Carlo simulations. The period and number of events used in the analysis are indicated in the lower part of each panel.
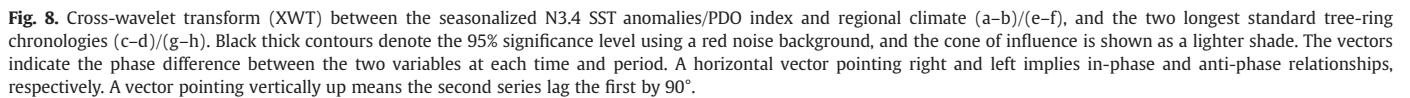
the suitability of many species for basic tree-ring analysis and dendroclimatology. Therefore this region has a high priority for tree-ring studies (Lara et al., 2005). In this paper we present the first analysis of climate signals from the tree-rings of three species (*K. angustifolia*, *P. cuneifolia* and *F. imbricata*) that are new to dendrochronology. These species are widely distributed through the Andes of the semiarid region and central Chile (Table 1). The growth of these species at our high elevation sampling sites is positively correlated with temperature but is mainly controlled by winter precipitation (Fig. 4), and similar to the regional climate, it is strongly modulated by conditions in the equatorial Pacific at both interannual and interdecadal timescales (Figs. 4 and 8a–d).

The highly significant statistics of interannual variability and common signal in our chronologies (Table 2) are comparable to those found in other arid and semiarid regions (Boninsegna, 1992). For instance, high values of mean sensitivity from 0.4 to 0.85 have also been found in arid or semiarid regions of North America (Fritts, 1974),

Asia (Liang et al., 2001) and in subtropical desert species in northern and central Peru (López et al., 2005; 2006; Rodríguez et al., 2005), and in *Prosopis chilensis* in the lowlands of our study area (López et al., 2006). Likewise, similar responses to winter precipitation have been typically found in other tree-ring studies along the Andes of central Chile under the Mediterranean-type climate (LeQuesne, 1999). Indeed, high-quality multi-centennial precipitation reconstructions using tree-rings from relict populations of the conifer *Austrocedrus chilensis* have been developed for Santiago de Chile (Boninsegna, 1988; LeQuesne et al., 2009-this issue) and also for the entire region of central Chile between 30° and 35°S (LeQuesne et al., 2006). However, poor and insignificant responses to precipitation have been reported for *Prosopis chilensis* in the lowlands of our sampling area (López et al., 2006), although using a tree-ring series with low common signal. Our results contrast with those of tree-ring studies of some riparian shrub species at similar latitudes and elevations in the semiarid Andes of Argentina, where summer temperature is the main factor controlling tree growth because of the relatively stable water supply (Roig et al., 1988; Schmelter, 1999). Nevertheless, as in our study area, precipitation is the main limiting factor for the radial growth of shrubs growing in the high-altitude drylands of the Argentinean Andes (Roig and Boninsegna, 1990). In the central Andes of Chile, significant but negative responses to high spring–summer temperatures have been found, together with positive responses to precipitation, in xeric tree-line sites of *Austrocedrus chilensis* at ~34°S (LeQuesne et al., 2000) and the northernmost tree-line populations of *Nothofagus pumilio* (southern beech) at 35°36′S (Lara et al., 2001). Higher spring–summer temperatures increase evapotranspiration and reduce soil water availability. The opposite responses to temperature of these two temperate species relative to our subtropical species (especially *K. angustifolia* and *P. cunefolia*) seem to be related to differences in the life history traits (e.g. ecophysiological traits).

In general, tree growth follows the regional climate rhythms (Fig. 3) but the strongest responses occur at the intraregional scale (Fig. 5). The chronologies closely follow the interannual and decadal climate variability. Nevertheless, despite the high correlation with precipitation the longest tree-ring chronologies (*K. angustifolia* and *P. cuneifolia*) do not exhibit any clear long-term trend (Fig. 3) as observed in the long precipitation records from central Chile, including La Serena and Santiago (Houghton et al., 2001; Quintana, 2004). However, the *K. angustifolia* chronology captures the strong interdecadal oscillation observed in the climate records during the wet period before 1920, although there is an antiphase relationship (Figs. 3 and 8c). This unexpected relationship could be related to a fire disturbance that temporarily altered the growth patterns at this site or simply to the weak correlation between the *K. angustifolia* chronology and precipitation at the La Serena station (Fig. 5 and Table 2), which is the only record of precipitation before 1907 (Fig. 3).

The climate of the semiarid region and central Chile is very sensitive to conditions in the equatorial Pacific (Montecinos and Aceituno, 2003; Garreaud et al., 2009-this issue). This strong influence of the tropical Pacific also leaves its imprint in tree growth at the interannual timescale. Our results agree with previous climatic and hydrometeorologic studies showing a strong ENSO-driven interannual variability where the warm El Niño events are associated with wet and warm conditions as opposed to cold La Niña events (e.g. Rutlland and Fuenzalida, 1991; Montecinos and Aceituno, 2003; Masiokas et al., 2006; Garreaud et al., 2009-this issue). However, our wavelet analysis (Figs. 6 and 8) reveals that the equatorial Pacific can also modulate the regional climate variability and hence tree growth at the interdecadal scale as shown by a coherent in-phase relationship. This means that interdecadal warm (cold) sea surface conditions are associated with warm (cold) and wet (dry) climate conditions and increased (reduced) tree growth in the semiarid region at the same timescale, analogous to the interannual El Niño and La Niña episodes. Nevertheless, during the 130 years of the instrumental record this low-

Fig. 8. Cross-wavelet transform (XWT) between the seasonalized N3.4 SST anomalies/PDO index and regional climate (a–b)/(e–f), and the two longest standard tree-ring chronologies (c–d)/(g–h). Black thick contours denote the 95% significance level using a red noise background, and the cone of influence is shown as a lighter shade. The vectors indicate the phase difference between the two variables at each time and period. A horizontal vector pointing right and left implies in-phase and anti-phase relationships, respectively. A vector pointing vertically up means the second series lag the first by 90°.

frequency signal is quite localized and is restricted only to a bidecadal band between 1870 and 1920 but it was strong enough to produce extreme and sustained wet conditions in the region, especially when coupled with El Niño events. Interestingly, long-term changes in the intensity and position of the subtropical anticyclone together with an increased frequency of El Niño events were observed in this same period (Aceituno et al., 1993), indicating an El Niño-like atmospheric teleconnection. Cross-spectral analyses indicate that this bidecadal signal is not related to the PDO mode, which is one of the most important ENSO-like modes acting at these timescales, especially in the North Pacific (Mantua et al., 1997; Garreaud and Battisti, 1999; Mantua and Hare, 2002). This signal can be related to the Interdecadal Pacific Oscillation (IPO), a Pacific-wide ENSO-like mode acting at

interdecadal and multidecadal timescales (Power et al., 1999; Folland et al., 2002; Linsley et al., 2005). The IPO is almost the Pacific-wide manifestation of the PDO of Mantua et al. (1997), but with as much variance in the Southern Pacific southward to at least 55°S as in the Northern Pacific producing some likely independent features. Global studies relating land rainfall with low-frequency ENSO-like modes (e.g. Allan, 2000; Meinke et al., 2005) show that the IPO is significantly and positively correlated with precipitation in central Chile. They also reveal that the classical ENSO sensitive areas, as our study region, are usually those that experience more low-frequency climate variability. A similar relationship between the IPO and precipitation in central Chile was found by Quintana (2004). However, additional work is necessary to assess the specific influences of the IPO

on the climate of north-central and central Chile and whether it captures the bidecadal signal observed in the Niño 3.4 region.

This study suggests a high potential of three new species for dendrochronological studies in the semiarid region of Chile, given their well-defined tree-rings, wide geographic distribution, good crossdating and strong climatic signals. The most promising species for dendroclimatic studies is *K. angustifolia* which has the potential to fill the gap in the tree-ring network between the northernmost populations of *Austrocedrus chilensis* (32°40′ S; LeQuesne et al., 2006) and *Nothofagus pumilio* (35°36′ S; Lara et al., 2001) in central Chile, because it is a widely distributed species growing at the tree-line through the region. Well-preserved remnant wood from dead *K. angustifolia* trees can be used to extend the chronologies into the past, covering the last 200–250 years. This would provide an important proxy record for precipitation and potentially also for temperature variability at high elevations, where few and short climate records are available.

Acknowledgements

References

Aceituno, P., 1988. On the functioning of the southern oscillation in the South American sector. Part I: surface climate. Mon. Weather Rev. 116, 505–524.

Aceituno, P., Fuenzalida, H., Rosenblüth, B., 1993. Climate along the extratropical west coast of South America. In: Mooney, H., Fuentes, E., Kronberg, B. (Eds.), Earth systems responses to global change: Contrasts between North and South America. Academic Press, San Diego, pp. 61–69.

Akaike, H., 1974. A new look at the statistical model identification. IEEE Trans. Automat. Contr. AC19 (6), 716–723.

Alexandersson, A., 1986. A homogeneity test applied to precipitation data. Int. J. Climatol. 6, 661–675.

Aljaro, M.E., Avila, G., Hoffmann, A., Kummerow, J., 1972. The annual rhythm of cambial activity in two woody species of the Chilean "matorral". Am. J. Bot. 59 (9), 879–885.

Allan, R.J., 2000. ENSO and climatic variability in the past 150 years. In: Diaz, H.F., Markgraf, V. (Eds.), El Niño and the Southern Oscillation: multiscale variability and its impacts on natural ecosystems and society. Cambridge Univ. Press, Cambridge, pp. 3–55.

Almeyda, E., Sáez, F., 1958. Recopilación de datos climáticos de Chile y mapas sinópticos respectivos. Ministerio de Agricultura, Santiago de Chile.

Argollo, M., Soliz, C., Villalba, R., 2004. Potencialidad dendrocronológica de *Polylepis tarapacana* en los Andes centrales de Bolivia. Ecol. Boliv. 39, 5–24.

Armesto, J.J., Arroyo, M.T.K., Hinojosa, L.F., 2007. The mediterranean environment of Central Chile. In: Veblen, T.T., Young, K.R., Orme, A.R. (Eds.), The physical geography of South America. Oxford Univ. Press, Oxford, pp. 184–199.

Arroyo, M.T.K., Squeo, F.A., Armesto, J.J., Villagrán, C., 1988. Effects of aridity on plant diversity in the northern Chilean Andes: results of a natural experiment. Ann. Miss. Bot. Gard. 75, 55–78.

Boninsegna, J.A., 1988. Santiago de Chile winter rainfall since 1220 as being reconstructed by tree rings. Quat. South Am. Antarct. Penins. 6, 67–87.

Boninsegna, J.A., 1992. South American dendroclimatological records. In: Bradley, R.S., Jones, P.D. (Eds.), Climate since A.D. 1500. Routledge, London, pp. 446–462.

Boninsegna, J.A., Villalba, R., Amarilla, L., Ocampo, J., 1989. Studies on tree rings, growth rates and age–size relationships of tropical trees in Misiones, Argentina. IAWA Bull. 10 (2), 161–169.

Briffa, K.R., 1995. Interpreting high-resolution proxy climate data: the example of dendroclimatology. In: Von Storch, H., Navarra, A. (Eds.), Analysis of Climate Variability: Applications of Statistical Techniques. Springer, Berlin, pp. 77–94.

Brohan, P., Kennedy, J.J., Haris, I., Tett, S.F.B., Jones, P.D., 2006. Uncertainty estimates in regional and global observed temperature changes: a new dataset from 1850. J. Geophys. Res. 111, D12106. doi:10.1029/2005JD006548.

Christie, D.A., Lara, A., Barichivich, J., Villalba, R., Morales, M., Cuq, E. 2009. El Niño-Southern Oscillation signal in the world's highest-elevation tree-ring chronologies from the Altiplano, Central Andes. Palaeogeogr. Palaeoclimatol. Palaeoecol. 281, 309–319 (this issue).

Cook, E.R., 1985. A time series analysis approach to tree-ring standardization. Ph.D. Thesis, Univ. of Arizona, Tucson, USA.

Cook, E.R., Kairiukstis, L.A., 1990. Methods of dendrochronology: applications in the environmental sciences. Kluwer, Dordrecht.

Cook, E.R., Krusic, P.J., 2006. Program ARSTAN: a tree-ring standardization program based on detrending and autoregressive time series modeling, with interactive graphics. Tree-Ring Laboratory, Lamont Doherty Earth Observatory. Columbia Univ., Palisades, N.Y.

Cook, E., Briffa, K., Meko, D., Graybill, D., Funkhouser, G., 1995. The 'segment length curve' in long tree-ring chronology development for palaeoclimatic studies. The Holocene 5, 229–237.

Dawdy, D.R., Matalas, N.C., 1964. Statistical and probability analysis of hydrologic data, part III. Analysis of variance, covariance, and time series. In: Chow, V.T. (Ed.), Handbook of Applied Hydrology. A Compendium of Water-Resources Technology. McGraw-Hill, pp. 8.68–8.90.

Folland, C.K., Renwick, J.A., Salinger, M.J., Mullan, A.B., 2002. Relative influences of the interdecadal Pacific oscillation and ENSO on the South Pacific convergence zone. Geophys. Res. Lett. 29 (13), 211–214.

Fritts, H.C., 1974. Relationships of ring widths in arid site conifers to variations in monthly temperature and precipitation. Ecol. Monogr. 44, 411–440.

Fritts, H.C., 1976. Tree rings and climate. Academic Press, London.

Gajardo, R., 1994. La vegetacion natural de Chile. Editorial Universitaria, Santiago de Chile.

Garreaud, R., Battisti, D., 1999. Interannual (ENSO) and interdecadal (ENSOlike) variability in the southern hemisphere tropospheric circulation. J. Climate 12, 2113–2123.

Garreaud, R.D., Aceituno, P., 2007. Atmospheric circulation over South America: mean features and variability. In: Veblen, T.T., Young, K.R., Orme, A.R. (Eds.), The physical geography of South America. Oxford Univ. Press, Oxford, pp. 45–59.

Garreaud, R., Vuille, M., Compagnucci, R., Marengo, J. 2009. Present-day South American climate. Palaeogeogr. Palaeoclimatol. Palaeoecol. 281, 180–195 (this issue).

Ghil, M., Allen, R.M., Dettinger, M.D., Ide, K., Kondrashov, D., Mann, M.E., Robertson, A., Saunders, A., Tian, Y., Varadi, F., Yiou, P., 2002. Advanced spectral methods for climatic time series. Rev. Geophys. 40 (1), 1.1–1.41.

Grinsted, A., Moore, J.C., Jevrejeva, S., 2004. Application of the cross wavelet transform and wavelet coherence to geophysical time series. Nonlinear Process. Geophys. 11, 561–566.

Holmes, R.L., 1983. Computer-assisted quality control in tree-ring dating and measurements. Tree-Ring Bull. 43, 69–75.

Holmes, R., Swetnam, T., 1994. Program event user's manual. Superposed epoch analysis in fire history studies. Laboratory of Tree-Ring Research. University of Arizona, Tucson, AZ.

Holmgren, M., Scheffer, M., Ezcurra, E., Gutiérrez, J.R., Mohren, G.M.J., 2001. El Niño effects on the dynamics of terrestrial ecosystems. Trends Ecol. Evol. 16, 89–94.

Holmgren, M., Stapp, P., Dickman, C.R., Gracia, C., Graham, S., Gutiérrez, J.R., Hice, C., Jaksic, F., Kelt, D.A., Letnic, M., Lima, M., López, B.C., Meserve, P.L., Milstead, W.B.G., Polis, A., Previtali, M.A., Richter, M., Sabaté, S., Squeo, F.A., 2006. A synthesis of ENSO effects on drylands in Australia, North America and South America. Adv. Geosci. 6, 69–72.

Houghton, J.T., Ding, Y., Griggs, D.J., Noguer, M., van der Linden, P.J., Dai, X., Maskell, K., Johnson, C.A., 2001. Climate Change: The Scientific Basis. Cambridge Univ. Press, Cambridge, p. 881.

Hurrell, J.W., James, J., Hack, J., Shea, D., Caron, J.M., Rosinski, J., 2008. A new sea surface temperature and sea ice boundary data set for the Community Atmosphere Model. J. Climate. 21, 5145–5153.

Jevrejeva, S., Moore, J.C., Grinsted, A., 2003. Influence of the Arctic oscillation and El Niño-southern oscillation (ENSO) on ice conditions in the Baltic Sea: the wavelet approach. J. Geophys. Res. 108, 4677. doi:10.1029/2003JD003417.

Jones, P.D., Hulme, M., 1996. Calculating regional climatic time series for temperature and precipitation: methods and illustrations. Int. J. Climatol. 16, 361–377.

Lara, A., Aravena, J.C., Wolodarsky, A., Villalba, R., Luckman, B.H., Wilson, R., 2001. Dendroclimatology of high-elevation *Nothofagus pumilio* forests in the Central Andes of Chile. Can. J. For. Res. 31, 925–936.

Lara, A., Wolodarsky-Franke, A., Aravena, J.C., Villalba, R., Solari, M.E., Pezoa, L., Rivera, A., Le Quesne, C., 2005. Climate fluctuations derived from treerings and other proxy-records in the Chilean Andes: state of the art and future prospects. In: Huber, U.M., Bugmann, H.K., Reasoner, M.A. (Eds.), Global Change and Mountain Regions. An overview of current knowledge. Springer, Dordrecht, pp. 145–156.

LeQuesne, C., 1999. Dendrochronology of *Austrocedrus chilensis* (D. Don) Pic. Ser. et Bizz. (*Cupressaceae*), in the northern limit of distribution, Chile (in Spanish). Ph.D. Thesis, Universidad de Oviedo, Spain.

LeQuesne, C., Aravena, J.C., Alvarez-García, M.A., Fernández-Prieto, J.A., 2000. Dendrocronología de *Austrocedrus chilensis* en Chile Central. In: Roig, F. (Ed.),

Dendrocronología en América Latina. Editorial Nacional de Cuyo, Mendoza, pp. 159–175.

LeQuesne, C., Stahle, D.W., Cleaveland, M.K., Therrell, M.D., Aravena, J.C., Barichivich, J., 2006. Ancient *Austrocedrus* tree-ring chronologies used to reconstruct central Chile precipitation variability from A.D. 1200 to 2000. J. Climate 19, 5731–5744.

LeQuesne, C., Acuña, C., Boninsegna, J., Rivera, A., Barichivich, J. 2009. Long-term glacier variations in central Andes of Argentina and Chile, inferred from historical records and tree-ring reconstructed precipitation. Palaeogeogr. Palaeoclimatol. Palaeoecol. 281, 334–344 (this issue).

Liang, E., Shao, X., Hu, Y., Lin, J., 2001. Dendroclimatic evaluation of climate-growth relationships of Meyer-spruce (*Picea meyeri*) on a sandy substrate in semi-arid grassland, north China. Trees 15, 230–235.

Linsley, B.K., Wellington, G.M., Schrag, D.P., Ren, L., Salinger, M.J., Tudhope, A.W., 2005. Geochemical evidence from corals for changes in the amplitude and spatial pattern of South Pacific interdecadal climate variability over the last 300 years. Clim. Dyn. 22, 1–11.

López, B.C., Sabaté, S., Gracia, C.A., Rodríguez, R., 2005. Wood anatomy of *Prosopis pallida* H.B.K. from Peru and its suitability for dendrochronology. J. Arid Environ. 61, 541–554.

López, B.C., Rodríguez, R., Gracia, C.A., Sabaté, S., 2006. Climatic signals in growth and its relation to ENSO events of two *Prosopis* species following a latitudinal gradient in South America. Glob. Chang. Biol. 12, 897–906.

Luckman, B.H., Boninsegna, J.A., 2001. The assessment of present, past and future climate variability in the Americas from treeline environments. PAGES Newsl. 9, 17–19.

Mantua, N.J., Hare, S.R., 2002. The Pacific decadal oscillation. J. Oceanogr. 58, 35–44.

Mantua, N.J., Hare, S.R., Zhang, Y., Wallace, J.M., Francis, R.C., 1997. A Pacific interdecadal climate oscillation with impacts on salmon production. Bull. Am. Meteorol. Soc. 78, 1069–1079.

Masiokas, M.H., Villalba, R., Luckman, B.H., LeQuesne, C., Aravena, J.C., 2006. Snowpack variations in the central Andes of Argentina and Chile, 1951–2005: large-scale atmospheric influences and implications for water resources in the region. J. Climate 19, 6334–6352.

Meinke, H., deVoil, P., Hammer, G., Power, S., Allan, R., Stone, R., Folland, C., Potgieter, A., 2005. Global decadal rainfall variability: signal or noise? J. Climate 18, 89–96.

Miller, A., 1976. The climate of Chile. In: Schwerdtfeger, W. (Ed.), World Survey of Climatology. Climates of Central and South America. Elsevier, Amsterdam, The Netherlands, pp. 113–131.

Montecinos, A., Aceituno, P., 2003. Seasonality of the ENSO related rainfall variability in central Chile and associated circulation anomalies. J. Climate 16, 281–296.

Morales, M.S., Villalba, R., Grau, H.R., Villagra, P.E., Boninsegna, J.A., Ripalta, A., Paolini, L., 2001. Potencialidad de *Prosopis ferox* Griseb (Leguminosae, subfamilia: Mimosoideae) para estudios dendrocronológicos en desiertos subtropicales de alta montaña. Rev. Chil. Hist. Nat. 74, 889–896.

Morales, M., Villalba, R., Grau, H.R., Paolini, L., 2004. Rainfall-controlled tree growth in high-elevation subtropical treelines. Ecology 85, 3080–3089.

Moya, J., 2006. Desarrollo de las primeras cronologías de Queñoa (*Polylepis tarapacana* Phil.) en el Altiplano de la Región de Tarapacá, Chile. M.Sc. Thesis, Facultad de Ciencias Forestales, Univ. Austral, Chile.

Piper, F.I., Caviares, L.A., Reyes-Diaz, M., Corchera, L.J., 2006. Carbon sink limitation and frost tolerance control performance of the tree *Kageneckia angustifolia* D. Don (Rosaceae) at the treeline in central Chile. Plant Ecol. 185, 29–39.

Pittock, A.B., 1980. Patterns of climate variation in Argentina and Chile—I. Precipitation, 1931–1960. Mon. Weather Rev. 108, 1362–1369.

Power, S., Casey, T., Folland, C., Colman, A., Mehta, V., 1999. Inter-decadal modulation of the impact of ENSO on Australia. Clim. Dyn. 15, 319–324.

Quintana, J., 2004. Factors involved in the interdecadal precipitation variability in Chile (in Spanish). M.Sc. Thesis, Department of Geophysics, Univ. de Chile, Santiago, Chile.

Rodríguez, R., Mabres, A., Luckman, B.H., Evans, M., Masiokas, M., Ektvedt, M.K., 2005. "El Niño" events recorded in dry-forest species of the lowlands of northwest Peru. Dendrochronologia 22, 181–186.

Roig, F.A., Boninsegna, J.A., 1990. Environmental factors affecting growth of *Adesmia* communities as determined from tree rings. Dendrochronologia 8, 39–66.

Roig, F.A., Villalba, R., Ripalta, A., 1988. Climatic factors in *Discaria trinervis* growth in Argentine Central Andes. Dendrochronologia 6, 61–70.

Roig, F., Fernández, M., Gareca, E., Altamirano, S., Monge, S., 2001. Estudios dendrocronológicos en los ambientes húmedos de la Puna Boliviana. Rev. Bol. Ecol. Cons. Amb. 9, 3–13.

Rundel, P.W., 1981. The matorral zone of central Chile. In: Di Castri, F., Goodall, D.W., Specht, R.L. (Eds.), Ecosystems of the world, 11. Mediterranean-type shrublands. Elsevier, Amsterdam, pp. 175–201.

Rundel, P.E., Villagra, P.E., Dillon, M.O., Roig-Juñent, S., Debandi, G., 2007. Arid and semi-arid ecosystems. In: Veblen, T.T., Young, K.R., Orme, A.R. (Eds.), The physical geography of South America. Oxford Univ. Press, Oxford, pp. 158–183.

Rutlland, J., Fuenzalida, H., 1991. Synoptic aspects of the central Chile rainfall variability associated with the Southern Oscillation. Int. J. Climatol. 11, 63–76.

Schmelter, A., 1999. The temperature-growth relationship of *Discaria trinervis* in the central Andes of Argentina (33–35°S) and the influence of local site factors. Dendrochronologia 17, 87–98.

Schulman, E., 1956. Dendroclimatic changes in semiarid America. Univ. of Arizona Press, Tucson, AZ.

Soliz, C., Villalba, R., Argollo, J., Morales, M.S., Christie, D.A., Moya, J., Pacajes, J. 2009. Spatial - temporal variations in *Polylepis tarapacana* growth across the Bolivian Altiplano during the 20th century. Palaeogeogr. Palaeoclimatol. Palaeoecol. 281, 296–308 (this issue).

Štěpánek, P., 2005. AnClim — software for time series analysis. Fac. of Natural Sciences. Masaryk University, Brno, Tschek Republic.

Stokes, M.A., Smiley, T.L., 1968. An introduction to tree-ring dating. Univ. of Chicago Press, Chicago, IL.

Squeo, F.A., Arancio, G., Gutiérrez, J.R., 2001. Libro Rojo de la Flora Nativa de la Región de Coquimbo y de los Sitios Prioritarios para su Conservación. Ediciones de la Universidad de La Serena, La Serena, Chile.

Torrence, C., Compo, G.P., 1998. A practical guide to wavelet analysis. Bull. Am. Meteorol. Soc. 79, 61–78.

Trenberth, K.E., 1997. The definition of El Niño. Bull. Am. Meteorol. Soc. 78, 2771–2777.

Van Husen, C., 1967. Klimagliederung in Chile auf der Basis von Häufigkeitsverteilungen der Niederschlagssummen. Freibg. Geogr. Hefte 4, 1–113.

Villalba, R., 2000. Dendroclimatology: a southern hemisphere perspective. In: Smolka, P.P., Volkheimer, W. (Eds.), Southern hemisphere paleo- and neoclimates. Springer, Berlin, Germany, pp. 27–57.

Villalba, R., Boninsegna, J.A., Holmes, R.L., 1985. *Cedrela angustifolia* and *Juglans australis*: Two new tropical species useful in dendrochronology. Tree-Ring Bull. 45, 25–36.

Villalba, R., Boninsegna, J.A., Ripalta, A., 1987. Climate, site conditions and tree-growth in subtropical northwestern Argentina. Can. J. For. Res. 17 (12), 1527–1544.

Villalba, R., Holmes, R.L., Boninsegna, J.A., 1992. Spatial patterns of climate and tree growth variations in subtropical northwestern Argentina. J. Biogeogr. 19, 631–649.

Villalba, R., Grau, H.R., Boninsegna, J.A., Jacoby, G., Ripalta, A., 1998. Tree-ring evidence for long term precipitation changes in subtropical South America. Int. J. Climatol. 18, 1463–1478.

Villalba, R., D'Arrigo, R.D., Cook, E.R., Wiles, G., Jacoby, G.C., 2001. Decadal-scale climatic variability along the extratropical western coast of the Americas: evidences from tree-ring records. In: Markgraf, V. (Ed.), Inter-Hemispheric Climate Linkages. Academic Press, San Diego, pp. 155–172.

Villalba, R., Luckman, B.H., Boninsegna, J., D'Arrigo, R.D., Lara, A., Villanueva-Diaz, J., Masiokas, M., Argollo, J., Soliz, C., LeQuesne, C., Stahle, D., Roig, F., Aravena, J.C., Hughes, M.K., Wiles, G., Jacoby, G., Hartsough, P., Wilson, R.J.S., Watson, E., Cook, E.R., Cerano-Paredes, J., Therrell, M., Cleaveland, M., Morales, M.S., Salzer, M., Moya, J., Pacajes, J., Massacchesi, G., Biondi, F., Urrutia, R., Martinez Pastur, G., in press. Dendroclimatology from regional to continental scales: Understanding regional processes to reconstruct large-scale climatic variations across the Western Americas. In: Hughes, M., Diaz, H., Swetnam, T. (Eds.), Tree Rings and Climate: Sharpening the Focus. Advances in Global Change Research. Springer, Berlin.

Vuille, M., Amman, C., 1997. Regional snowfall patterns in the high, arid Andes. Clim. Change 36, 413–423.

Wigley, T.M., Briffa, K.R., Jones, P.D., 1984. On the average value of correlated time series with applications in dendroclimatology and hydrometeorology. J. Clim. Appl. Meteorol. 23, 201–213.